Characterising Sediment Transport Capacity on Hillslopes Using Hypsometric Functions

I. P. Prosser, J. Gallant and P. Rustomji

CSIRO Land and Water and Cooperative Research Centre for Catchment Hydrology, GPO Box 1666, Canberra, ACT 2601, Australia (ian.prosser@cbr.clw.csiro.au)

Abstract: Hypsometric curves are used by geomorphologists to describe the shape of the landscape. They are curves of the distribution of area with elevation in a landscape. A complimentary description is the belt width curve: the distribution of contour length with elevation. Hypsometric curves have been used qualitatively in relation to erosion processes. Here we show a formal relationship with sediment transport capacity on hillslopes and propose hypsometric functions and belt width functions as compound terrain indicators of erosion potential. The functions represent complex topography while retaining a hillslope scale indicator, rather than making calculations at the scale of each cell of a digital elevation model. By using the original contour elevations we avoid some of the artefacts of erosion modelling at the individual grid cell scale.

Keywords: Terrain analysis; Hillslopes; Sediment transport; Hypsometric functions

1. INTRODUCTION

Hillslope topography is one of the strongest influences on landscape patterns of sediment transport, but it can be difficult to characterise accurately because of its complex three dimensional geometry. The upslope catchment area at any point on a hillslope is a primary determinant of the flow discharge, and the local topography around the point determines the confinement or dispersion of the flow and the local energy gradient. These both control sediment transport by overland flow. Deposition, for example, can occur where gradient decreases or where flow disperses.

Several approaches have been used to characterise the effect of topography on sediment yields. The simplest methods treat hillslopes as planes or simple curves, specifying the length, average gradient, and simple shape of flow paths [e.g. Saleh et al., 2000]. These do not represent the complex three dimensional shapes of the land well but they are relatively easy to measure and incorporate into sediment transport algorithms. At the other end of the spectrum is detailed representation of topography through high resolution digital elevation models (DEMs) which are used to calculate local slope and planform and profile curvature [Moore et al., 1992]. Those attributes can then be used in detailed physically based models of erosion and deposition on each grid cell [e.g. Mitas and Mitasova 1998]. These methods represent topography well but can be computationally expensive and the process models are often hard to parameterise at fine spatial resolution.

A more significant problem is the representation of terrain by detailed DEMs. Erosion models are sensitive to errors in terrain curvature which arise from the interpolation of DEMs from contour data. The errors arise either from the original contour positioning or from the interpolation algorithms used to construct regular grids at fine spacing from irregularly spaced contour data [see Figures 2.8, 2.10, and discussion in Hutchinson and Gallant, 2000]. The errors can produce bands of local erosion, followed immediately downslope by deposition, in places where there is no field indication of such small-scale fluctuations. Furthermore, flow routing algorithms are used to compute upslope catchment area from regular grid DEMs but the predicted accumulation of area to each cell is sensitive to the choice of algorithm [Wilson et al., 2000].

Current concerns of sediment transport are often at the catchment and whole hillslope scales, involving issues such as sediment delivery to

streams and identification of target hillslopes for restoration. Prediction of sediment transport in individual grid cells is at a finer scale than is required, so if that resolution produces errors from terrain interpolation there is merit in considering larger scale approaches that still represent the complexity of natural terrain.

The method we present here represents topography on hillslopes using contour bands, the scale of the original terrain information. Two compound terrain attributes are constructed for each hillslope: the hypsometric function and the belt width function [Strahler 1952; Figure 1]. The hypsometric function measures the area above each contour on a hillslope. It is a commonly used catchment terrain attribute that we apply to individual hillslopes. Its shape is a function of gradient and planform and profile curvature. The hypsometric curve has been associated with erosion processes but here we present the first analytical solution of the relationship.

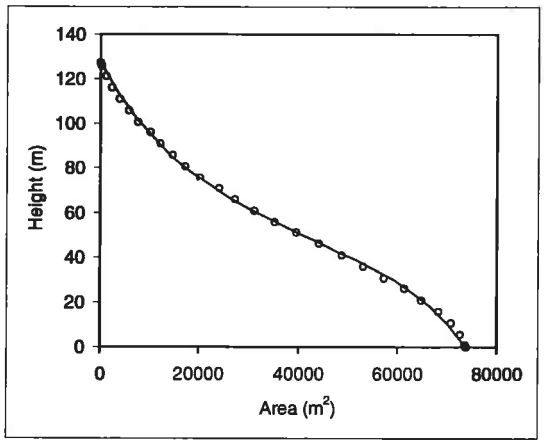

Figure 1. A hypsometric curve for a hillslope showing measurements at contours and the fit of (7).

The belt width function measures the changing length of contour as catchment area grows from the top to the foot of a hillslope. Combined with the hypsometric curve it allows planform and profile curvature to be separated. We show how the two functions can be incorporated into an equation for sediment transport capacity that is used in grid cell erosion modelling. The results are hillslope scale patterns of sediment transport capacity that use high resolution DEMs and represent complex topographic shapes but which avoid the grid-based algorithms for calculating terrain curvature and catchment area.

2. METHOD DEVELOPMENT

Almost all physically based models of sediment transport include a term for sediment transport capacity (STC), as an expression of the maximum load of sediment that flow can carry. If STC increases downslope there is increasing potential for erosion. If it decreases there is potential for sediment deposition.

STC (T, t/y) is predicted as a function of the applied discharge per unit width (q m^2/s) and local energy gradient approximated by the topographic gradient (S):

$$T = kq^{\beta}S^{\delta} \qquad (1)$$

where k, β and δ are empirical or theoretically derived constants. When applied to hillslopes, q is commonly proportional to upslope contributing area per unit width (A/w, m). Prosser and Rustomji [2000] reviewed relations for STC, finding median values of 1.4 for both β and δ. Thus (1) can be written as:

$$T = K(\frac{A}{w}S)^{1.4}. \qquad (2)$$

The constant K represents the non-topographic landscape characteristics that influence sediment transport capacity. By keeping K spatially constant, equation (2) becomes a purely topographic rule for evaluating sediment transport capacity across a landscape.

The potential, or maximum rate of erosion or deposition (E, m/y) must also obey conservation of mass which for a hillslope can be expressed as:

$$E = -\frac{\partial H}{\partial t} = \frac{1}{w}\frac{\partial (wT)}{\partial x} \qquad (3)$$

where H (m) is elevation, t is time (y), and x is horizontal position along a flow path (m). Treating a hillslope as a flow tube (Figure 2) relates S and ∂x to A:

$$S(A) = -\frac{\partial H}{\partial A}w \qquad (4)$$

and

$$\partial x = \frac{\partial A}{w} \qquad (5)$$

Substituting (2), (4) and (5) into (3) produces

$$E(A) = -1.4Kw\left(A\frac{\partial H}{\partial A}\right)^{0.4}\left(\frac{\partial H}{\partial A} + A\frac{\partial^2 H}{\partial A^2}\right) + K\frac{\partial w}{\partial A}\left(A\frac{\partial H}{\partial A}\right)^{1.4} \quad (6)$$

Equation (6) expresses erosion and deposition potential in terms of topography as represented by the hypsometric function [$H = f(A)$] and belt width function [$w = f(A)$]. We use A as the independent variable because the integral of $E(A)$ gives the maximum volume of sediment that can be exported from the hillslope. We could also have used H or x.

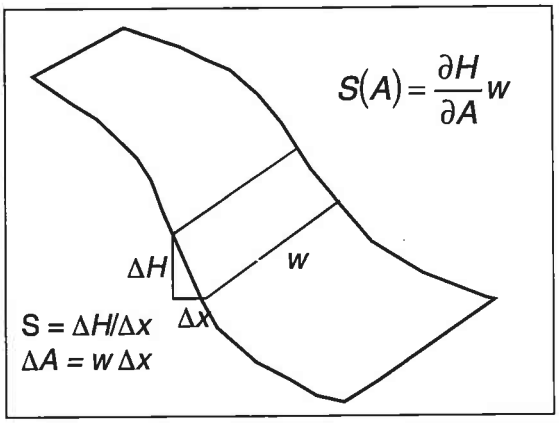

Figure 2. Definition of slope $S(A)$ and contour belt width (w).

To implement (6) requires differentiable functions for the hypsometric and belt width curves. We found that good fits to normalised hypsometric curves ($\eta = H/R$, where R = hillslope relief; and $\alpha = A/C$, where C = total hillslope area) were obtained from a function of the form:

$$\eta(\alpha) = \left(\frac{m}{k\alpha + m}\right)^m \left(\frac{l - l^{\alpha^n}}{l - 1}\right) \quad (7)$$

where k,l,m and n are curve fitting parameters.

The solution of (6) is based on the dimensional form of the hypsometric curve as actual values of upslope area and slope influence the intensity of erosion and deposition. Equation (7) is differentiated twice for substitution into (6).

We found that an exponential function fitted the belt width curve well for each hillslope:

$$w(\alpha) = s(1 + p\alpha)\left(1 - e^{-q\alpha}\right)\left(1 - e^{-r(1-\alpha)}\right) \quad (8)$$

where p,q,r and s are curve fitting parameters. This is differentiated for substitution into (6).

3. APPLICATION TO A CATCHMENT

The patterns of erosion and deposition that arise from hypsometric and belt width curves of hillslopes are illustrated by application to the Gungoandra Creek catchment on the Southern Tablelands of New South Wales (Figure 3). This is a 5 km^2 catchment with steep degraded hillslopes and a network of gullies. It was the subject of a study into the topographic limits of gully erosion [Prosser and Abernethy, 1996]. We used the digitised 5 m contour data of Prosser and Abernethy [1996] to construct a 10 m resolution regular grid DEM, using ANUDEM software [Hutchinson, 1989]. The mapped gullies were used to define a network of stream links defined by tributary nodes. These links were used to divide the catchment into 171 hillslope polygons, each draining to a particular stream link. The boundaries of hillslopes were defined by a program which delineates hydrological elements in a catchment based on smooth lines constructed in upslope directions for ridges and catchment divides and downslope directions for channels [Gallant, 1999]. Each first order stream has three hillslopes: the unchanneled hollow at the stream head, and hillslopes draining over the left and right banks of the stream link. Higher order streams have just left and right bank hillslopes.

Hypsometric curves were constructed for each hillslope polygon by summing the number of grid cells above the elevation of each of the raw contours used to construct the DEM. The data points on the raw hypsometric curves were then normalised. Equation (7) was fitted to the normalised points using an iterative curve fitting routine [Gnuplot, 2001]. This produced functions where the root mean square error was less than 3%.

The mean width was calculated from the DEM by using the finite difference form of (4) to measure the mean width between the raw contours, and (8) was fitted to these values as described above. The functions and their derivatives were then input into (6) to obtain erosion curves for each hillslope. To make the values of erosion broadly realistic we set K = 0.15, which erodes a 200 m long, planar hillslope of 10% gradient, at an average rate of 1 mm/y.

4. RESULTS

In Figure 4 we show examples of fitted hypsometric, belt width, and erosion curves to

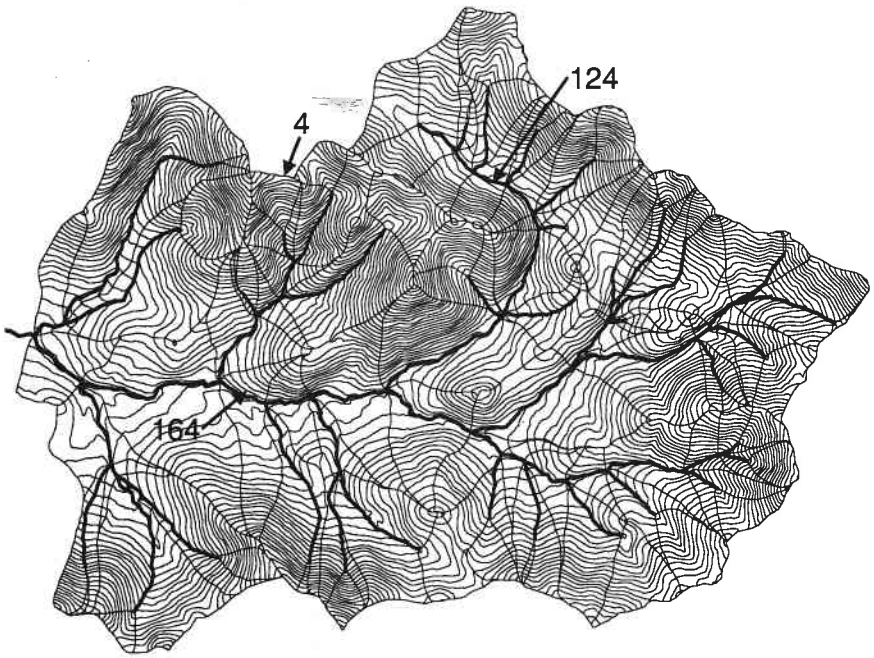

Figure 3. Map of Gungoandra Creek showing stream network, 5 m contours, and hillslope sub-catchments. Numbered hillslopes are those shown in Figure 4.

illustrate the range of patterns found. Hillslope 4 (Figure 3) is a typical curve for a hillslope hollow (the small unchannelled valley above the head of a first order stream). There is relatively low erosion toward the top of the hillslope, where flow spreads out, shown by increasing contour width. There is a sharp increase in erosion potential at the foot of the hillslope, where a large contributing area concentrates into a narrow hollow of steep gradient, conditions which maximise erosion potential. Under this topography, the lower part of the hypsometric curve has a high slope and is convex up, indicating low and decreasing increments of contributing area as elevation decreases.

Hillslope 124 is an example of a rectangular hillslope draining over the side of a stream (Figure 3). In general, rates of erosion from lateral hillslopes are low in comparison with those from hillslope hollows, for the planforms of these hillslopes are either divergent or planar. Relatively high erosion potential occurs on the steep middle slope of hillslope 124 but the gradient decreases sharply near the bottom reducing the transport capacity and resulting in potential for deposition (negative erosion potential) (Figure 4). The hypsometric curve has a low gradient and a concave form over much of its length, and contour width is constant over much of the hillslope.

The third main type of hillslope is divergent in planform as illustrated by hillslope 164 (Figures 3 and 4). This has the lowest erosion potential over the upper slope of the three shown because of its low gradient and flow that spreads out. This is illustrated by a strongly concave, low gradient hypsometric curve and increasing contour width over much of the hillslope.

Hillslope 164 is predicted to have a sharp increase in erosion at the slope foot, much like a hillslope hollow. Many hillslopes draining over streams have this feature. It is most pronounced where the stream link has a significant gradient, intersecting with several contours at an oblique angle. The analysis presented so far assumes that the incremental area with a drop in elevation represents the area through which runoff drains. Where the stream intersects the lower contours obliquely there is only a small increment of area for each drop of elevation, suggesting that the flow converges, resulting in a high erosion potential. In reality, overland flow is not confined by the stream. Instead, flow passes into the stream and not onto the hillslope below. Thus, below the upper elevation of the stream link there is a gradual loss of overland flow into the stream so that as the foot of the stream link is approached the direct contribution from the hillslope approaches zero.

Over the short distances of an individual link, upland streams have a uniform gradient, so that it is reasonable to assume that there is a linear addition of hillslope runoff along the stream link. This loss of flow, or contributing area, to the

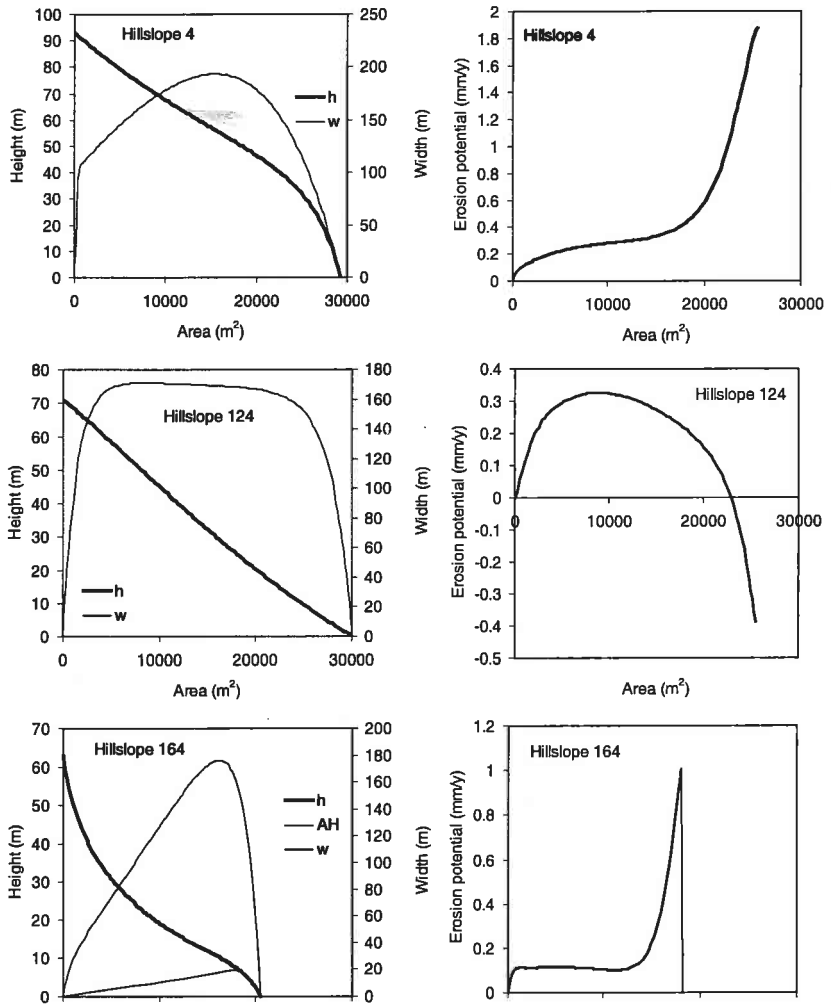

Figure 4. Fitted hypsometric and belt width functions and resultant erosion curves for three hillslopes at Gungoandra Creek. The correction for area lost to the stream is shown for Hillslope 164.

stream needs to be subtracted from the total contributing area used to calculate the erosion potential. Below the upper elevation of the stream link (H_1) the total upslope contributing area (A) is composed of that contributed to the stream (A_s) and that of the hillslope (A_H):

$$A = A_H + A_s \text{, for } H < H_1. \quad (9)$$

At any elevation $H < H_1$, a linear increase in A_s along the stream gives

$$A_s = A\left(\frac{H_1 - H(A)}{H_1}\right), \text{ for } H < H_1. \quad (10)$$

Combining (9) and (10) and modifying (6) in terms of A_H gives

$$E(A) = -1.4Kw\left(A_H \frac{\partial H}{\partial A}\right)^{0.4}\left(\frac{\partial H}{\partial A}\frac{\partial A_H}{\partial A} + A_H \frac{\partial^2 H}{\partial A^2}\right) + K\frac{\partial w}{\partial A}\left(A_H \frac{\partial H}{\partial A}\right)^{1.4}, \text{ for } H < H_1. \quad (11)$$

(11) includes one extra term to those of (7):

$$\frac{\partial A_H}{\partial A} = 1 - \left(\frac{h_1 - h(A) - A\frac{\partial h}{\partial A}}{h_1}\right), \text{ for } H < H_1. \quad (12)$$

Applying (12) removes the increasing erosion potential at the base of most lateral hillslopes. The correction causes erosion potential to approach zero at the lowest elevation of the hillslope, as hillslope area approaches zero at that point. In some cases, such hillslope 164, a significant rise in erosion potential at the slope base remains (Figure 4). This occurs where contours close to each other and the stream create relatively high gradients at the slope foot and where there is subsequent exaggeration in the

shape and extent of the convex foot to the hypsometric curve. Consequently predictions in the bottom 5-10% of the slope may not be reliable and require improvements to DEM production and curve fitting.

5. CONCLUSIONS

In using hypsometric and belt width curves to predict sediment transport potential on hillslopes we have developed a compound terrain indicator of the influence of hillslope topography on erosion, deposition and sediment yield potential. Hypsometric and belt width curves capture the complex shapes of hillslopes in greater detail than is possible using geometric shapes or hillslope profiles, while still being an overall summary of the hillslope shape and erosion response. Hypsometric curves are amenable to classifying hillslopes into differing types of sediment behaviour and of representing both erosion and deposition.

High resolution grid-based DEMs capture more details of topography but produce results at a finer scale than hillslopes. The influence of topography on sediment transport is usually of interest at the landscape scale, covering issues such as predictions of catchment sediment yields and sources of sediment. Hillslopes probably represent the finest scale of interest for these applications, hence their use as the terrain unit in most catchment models.

A further reason for focussing terrain analysis at the hillslope scale is that the analysis is conducted at the level of measurement of the original topographic information. Grid-based DEMs are generally constructed from contour data. While we used a DEM to construct the hypsometric curves we capture the information at the elevation of the original contours. This reduces the reliance on the surface interpolation techniques that are used to model elevation between contours. Many of the problems of surface fitting to contours can be avoided by appropriate choice of grid resolution [Hutchinson and Gallant, 2000]. Some, however, derive from local errors in mapping of the original contours. These errors are enhanced in predictions of hillslope curvature on which grid cell sediment transport models are based. Hypsometric curves represent the average spacing of contours along a hillslope and are consequently less sensitive to local errors in contour position. In analysing the DEM at the original contour elevations there is less need to consider the artefacts of the choice of grid resolution. It is a more rational and parsimonious approach to proceed as directly as possible from the topographic information to sediment transport prediction.

6. REFERENCES

Gallant, J.C., Terrae: A New Element Network Tool for Hydrological Modelling, paper presented at Envirowater 99: Emerging Technologies for Sustainable Land Use and Water Management, (unpublished) 1999.

Gnuplot, http://www.gnuplot.org, 2001.

Hutchinson, M.F., A new procedure for gridding elevation and stream line data with automatic removal of pits, *Journal of Hydrology, 106,* 211-32, 1989.

Hutchinson, M.F. and J. C. Gallant, Digital elevation models and representation of terrain shape, In Wilson, J. P. and J. C. Gallant (eds) *Terrain Analysis*, 29-50, Wiley and Sons, New York, 2000.

Mitas, L. and H. Mitasova, Distributed soil erosion simulation for effective erosion prevention, *Water Resources Research, 34,* 505-516, 1998.

Moore, I.D., J. P. Wilson and C. A. Ciesiolka, Soil erosion prediction and GIS: linking theory and practice, paper presented at the International Conference on the Application of Geographic Information Systems to Soil Erosion Management, Toronto, Canada, 1992.

Prosser, I.P. and B. Abernethy, Predicting the topographic limits to a gully network using a digital terrain model and process thresholds, *Water Resources Research, 32,* 2289-2298, 1996.

Prosser, I.P. and P. Rustomji, Sediment transport capacity relations for overland flow, *Progress in Physical Geography, 24,* 179-93, 2000.

Saleh, A., J. G. Arnold, P. W. Gassman, L. M. Hauck, W. D. Rosenthal, J. R. Williams and A. M. S. McFarland, Application of SWAT for the Upper Bosque River Watershed, *American Society of Agricultural Engineeers, 43*(5), 1077-1087, 2000.

Strahler, A.N., Hypsometric (area-altitude) analysis of erosional topography, *Bulletin Geological Society of America, 63,* 1117-1142, 1952.

Wilson, J. P., P. l. Repetto and R. D. Snyder, Effect of data source, grid resolution and flow-routing method on computed topographic attributes. Chapter 5 in Wilson, J.P. and J. C. Gallant (ed), *Terrain Analysis: Principles and Applications*, 133-161, John Wiley and Sons, New York, 2000.